Two minimal-variable symplectic integrators for stochastic spin systems

Two minimal-variable symplectic integrators for stochastic spin systems

Sagy Ephrati [*] and Erik Jansson [†]
Department of Mathematical Sciences, Chalmers University of Technology and University of Gothenburg, 41296 Göteborg, Sweden

(Received 17 December 2024; accepted 15 April 2025; published 2 May 2025)

We present two symplectic integrators for stochastic spin systems, based on the classical implicit midpoint method. The spin systems are identified with Lie-Poisson systems in matrix algebras, after which the numerical methods are derived from structure-preserving Lie-Poisson integrators for isospectral stochastic matrix flows. The integrators are thus geometric methods, require no auxiliary variables, and are suited for general Hamiltonians and a large class of stochastic forcing functions. Conservation properties and convergence rates are shown for several single-spin and multispin systems.

DOI: 10.1103/PhysRevE.111.054201

I. INTRODUCTION

Geometric integration methods are widely applied in the simulation of physical systems with conserved quantities. Algorithms that retain geometric properties of the underlying differential equations often exhibit benefits over standard integration algorithms, such as improved stability and statistical accuracy in long-time simulations [1]. Simultaneously, stochasticity is frequently employed to model uncertainty due to unresolved or unknown physical processes. It is therefore natural to (i) introduce noise in a manner that preserves the geometric structure and (ii) consider numerical integrators that respect the underlying mathematical structure even in the presence of noise. This has spurred the development and analysis of stochastic geometric integrators; see e.g., Refs. [2–9].

In the current study, we present two symplectic integrators for stochastic atomistic spin dynamics. Spin systems describe atomic phenomena often observed at finite temperature [10], of which the fluctuations can be modeled by an external stochastically fluctuating field. These systems possess a geometric Lie-Poisson (LP) structure, which motivates the use of so-called transport noise [11] to enable stochastic modeling. For deterministic spin systems, several numerical symplectic numerical integrators have been developed, e.g., based on splitting techniques [12–14] or normalizing the vector field governing the dynamics [15]. The methods presented here are suited for simulation of both deterministic spin systems and spin systems with transport noise. Specifically, the numerical integrators are variants of the implicit midpoint method that are symplectic, universally implementable for a large class of Hamiltonians and stochastic forcing functions, and do not require any auxiliary variables.

[*]Contact author: sagy@chalmers.se
[†]Contact author: erikjans@chalmers.se

Deterministic classical spin systems are noncanonical Hamiltonian systems with phase space $(\mathbb{S}^2)^n$, i.e., the n-fold product of the two-sphere, where n is the number of spins. In more detail, for a given Hamiltonian $H \in C^\infty((\mathbb{S}^2)^n)$, a deterministic classical spin system is given by

$$\dot{s}_i = s_i \times \nabla_{s_i} H(s_1, \ldots, s_n), \tag{1}$$

where $i = 1, \ldots n$, ∇_{s_i} denotes the gradient with respect to s_i, and $\times$ denotes the conventional cross product in $\mathbb{R}^3$.

These systems may be rewritten as equations in the Lie algebras $\mathfrak{su}(2)$ or $\mathfrak{so}(3)$[1], from which the geometric properties of the governing equations become apparent. For the single-spin case, we consider $\mathbb{R}^3$ equipped with the rigid body bracket

$$[u, v] = v \times u,$$

where $u, v \in \mathbb{R}^3$. The Euclidean space $\mathbb{R}^3$ can be identified with the Lie algebras $\mathfrak{su}(2)$ or $\mathfrak{so}(3)$ such that $\times$ in $\mathbb{R}^3$ corresponds to the matrix commutator in these Lie algebras, as described in the Appendix. In other words, spin systems in $\mathbb{R}^3$ are equivalently formulated as isospectral LP systems in $\mathfrak{su}(2)$ or $\mathfrak{so}(3)$. Therefore, we may also consider a general deterministic LP system on $\mathfrak{su}(2)$ or $\mathfrak{so}(3)$ and write this as an LP system in $\mathbb{R}^3$,

$$\dot{s} = s \times \nabla_s H, \tag{2}$$

for a Hamiltonian $H \in C^\infty(\mathbb{R}^3)$ and initial value $s(0) = s_0$.

Lie-Poisson systems have a remarkable geometric structure [16]. Indeed, regardless of the choice of Hamiltonian, LP systems evolve on *coadjoint orbits*, i.e., the orbits of the coadjoint action of a Lie group on the dual of its Lie algebra. In the specific case of $\mathfrak{so}(3)$ or $\mathfrak{su}(2)$, the corresponding group acts by rotation and the coadjoint orbits are therefore spheres. Furthermore, the LP structure induces a symplectic form on

[1]We should technically identify $\mathbb{R}^3$ with the duals of the Lie algebras $\mathfrak{su}(2)$ and $\mathfrak{so}(3)$. However, we can readily identify these duals with the corresponding Lie algebras.

the coadjoint orbits, namely the standard symplectic form on $\mathbb{S}^2$. Thus, the evolution of the LP system (2) is constrained to the sphere with radius $\|s_0\|$. This property exactly corresponds to the conservation of the spin magnitude over time.

The formulation of a single-spin system as an LP system is straightforwardly extended to systems of n spins by repeating the above procedure n times. This yields an LP system on $(\mathfrak{su}(2))^n \cong \mathbb{R}^{3n}$ or $(\mathfrak{so}(3))^n \cong \mathbb{R}^{3n}$ so that for each spin $i = 1, \dots n$, we obtain the equation

$$\dot{s}_i = s_i \times \nabla_{s_i} H(\mathbf{s}), \tag{3}$$

where $C^\infty(\mathbb{R}^{3n}) \ni H = (H_1, \dots H_n)$. Throughout this paper, we adopt $\|s_i(0)\| = 1$ for simplicity. Henceforth, systems of the form (3) are what we refer to as deterministic spin systems. In particular, these flows are Hamiltonian on $(\mathbb{S}^2)^n$ and remain in this space, meaning that the magnitude of each spin is preserved. We now consider some examples of spin systems, largely following the survey [17].

(1) *Rigid bodies.* One of the simplest examples of a spin system is the rigid body, where the angular momentum evolves according to Eq. (3) with $H(s) = \sum_{i=1}^3 \frac{1}{2I_j} s_j^2$, where $I = (I_1, I_2, I_3)$ is the moment of inertia tensor of the rigid body. It is also possible to consider nonlinear perturbations of the above Hamiltonian, to obtain more intricate dynamical behavior.

(2) *Larmor precession.* The equation of motion of a magnetic moment s in a constant external magnetic field B, modeled as a vector in $\mathbb{R}^3$, evolves according to the *Larmor equation* given by

$$\dot{s} = \gamma s \times B, \tag{4}$$

where $\gamma \in \mathbb{R}$ is the *gyromagnetic ratio*. We see that Eq. (4) is obtained from Eq. (3) by setting $N = 1$ and $H(s) = \gamma B \cdot s$, so that $\nabla_s H = \gamma B$.

(3) *Landau-Lifshitz equation.* To ensure that Eq. (4) eventually aligns with the external magnetic field, Gilbert [18] suggested adding a dissipative term to Eq. (4), to obtain the Landau-Lifshitz (LL) equation for a single spin, which is given by

$$\dot{s} = \gamma s \times B - \alpha s \times (s \times B), \tag{5}$$

where α is a phenomenological damping constant. This system is an LP system with double-bracket dissipation [19].

(4) *Heisenberg spin chain and extension to higher dimensions.* The previous examples concerned single-spin dynamics. The extension to multispin systems involves interacting spins on lattices, which represent ferromagnetic materials [17]. A one-dimensional periodic lattice of spins with nearest-neighbor interactions is the Heisenberg spin chain. The dynamics of the corresponding system with n spins $\mathbf{s} = (s_1, \dots s_n)$, $s_{n+1} = s_1$, is governed by the Hamiltonian $H : (\mathbb{R}^3)^n \mapsto \mathbb{R}$,

$$H(\mathbf{s}) = J \sum_{i=1}^n s_i \cdot s_{i+1} + \sum_{i=1}^n B \cdot s_i, \tag{6}$$

where $B \in \mathbb{R}^3$ is the external magnetic field and J is a coupling constant. This Hamiltonian leads to an LP system (3) given by

$$\dot{s}_i = J s_i \times (s_{i-1} + s_{i+1}) + s_i \times B. \tag{7}$$

If $B = 0$, we note that $s_i \times (s_{i-1} + s_{i+1}) = s_i \times (s_{i-1} - 2s_i + s_{i+1})$, where $s_{i-1} - 2s_i + s_{i+1}$ is recognized as a finite difference approximation of the Laplacian. One may therefore also view Eq. (7) as a discretization of the *continuous Landau-Lifshitz equation*

$$\dot{s} = s \times \Delta s. \tag{8}$$

A modification of Eq. (7) is the inclusion of non-nearest neighbor interactions. For instance, the Hamiltonian in for the latter in one spatial dimension reads

$$H(\mathbf{s}) = J_{nn} \sum_{i=1}^N s_i \cdot s_{i+1} + J_{nnn} \sum_{i=1}^N s_i \cdot s_{i+2} + \sum_{i=1}^N B \cdot s_i. \tag{9}$$

Combining LL dynamics with such extended Heisenberg interactions enables the formation of spatial structures in the dynamics. For example, the spontaneous emergence of spatial structures in the alignment of spins was observed when including non-nearest neighbor interactions [20,21]. Alternatively, an extension is possible to two-dimensional spin lattices with Heisenberg interactions, which permit vortex motion [22,23], or to three-dimensional structures. Incorporating the Heisenberg interaction in higher-dimensional spin configurations gives rise to a more complicated Hamiltonian but does not alter its appearance in the governing equation (3).

II. STOCHASTIC SPIN SYSTEMS

Spin dynamics at finite temperature can be described by coupling the spin system to a thermal reservoir [24]. The interaction between the spin system and the reservoir can subsequently be modeled as a random force describing thermal fluctuations [25]. Below we provide a brief description of transport noise in spin systems and why it preserves the geometric structure of the governing equations.

Introducing stochasticity to spin systems arbitrarily may lead to undesired nonphysical behavior. For instance, consider the Larmor equation (4) with additive Itô noise to obtain

$$\mathrm{d}s = \gamma s \times B \mathrm{d}t + \Sigma \mathrm{d}W,$$

where $s(0)$ is deterministic and of unit norm, $W = (W_1, W_2, W_3)$ is a $\mathbb{R}^3$-valued Brownian motion, and Σ is a diagonal matrix. The evolution of $f(s) = \|s\|^2$, using Itô's lemma, is described by

$$\begin{aligned} \mathrm{d}f &= \gamma s \cdot (s \times B)\mathrm{d}t + \mathrm{Tr}(\Sigma^T \Sigma)\mathrm{d}t + s^T \Sigma \mathrm{d}W \\ &= \mathrm{Tr}(\Sigma^T \Sigma)\mathrm{d}t + s^T \Sigma \mathrm{d}W. \end{aligned}$$

As a consequence,

$$\mathbb{E}[\|s\|^2] = \|s_0\|^2 + \mathrm{Tr}(\Sigma^T \Sigma)t,$$

which means that the spin magnitude is expected to grow, and the solution immediately leaves the sphere. A similar, but somewhat more involved calculation also holds in general for LP systems with additive Itô noise; see e.g., [26].

Therefore, if it is important that the length of the spin vectors are preserved, stochasticity must be added in a way

that respects the geometric structure of spin systems. The solution is to add *transport noise* [11], which gives rise to spin systems of the form

$$\mathrm{d}s_i = s_i \times \left(a_i(\mathbf{s})\mathrm{d}t + \sum_{j=1}^{M} \sigma_j(s_i) \circ \mathrm{d}W^{i,j}(t) \right). \tag{10}$$

Here $W^{i,j}$ all are independent Brownian motions and $\sigma_j(s_i)$ are of the form $\nabla_{s_i} H_j(\mathbf{s})$ for some choice of *noise Hamiltonians* $H_j : \mathbb{R}^3 \to \mathbb{R}$, $j = 1, \dots M$. Further, $a_i(\mathbf{s}) = \nabla_{s_i} H(\mathbf{s}) - \alpha s_i \times \nabla_{s_i} H(\mathbf{s})$, where α is a damping parameter. We remark that the transport noise introduced in (10) has been studied before in the context of spin systems; see, e.g., [27,28]. In particular, transport noise constitutes a special case of multiplicative noise: the stochastic term enters the governing equations in the same way as the Hamiltonian; it hence *transports* the spin.

Stochastic differential equations given by (10) are guaranteed to remain on $(\mathbb{S}^2)^N$. Intuitively, this is because the cross product between s_i and both $a_i(\mathbf{s})$ and $\sigma_j(s_i)$ only affects the evolution of s_i tangential to the sphere. Geometrically, it is a consequence of the fact that the cross product coincides with the Lie bracket on $\mathfrak{su}(2)$ and $\mathfrak{so}(3)$, which leads to solutions that remain on the coadjoint orbit [5]. As a result, stochastic systems of the form (10) have similar geometric properties, such as preservation of spin magnitude, as their deterministic counterparts. The stochastic term in Eq. (10) is interpreted in the Stratonovich sense, since manifold-valued curves can be extended to manifold-valued processes in differential geometry due to the ordinary chain rule for Stratonovich processes [29,30]. That is, if one would interpret (10) in the Itô sense, the desired conservation properties of the equations would be lost. Simultaneously, it is possible to rewrite the Stratonovich formulation to an Itô formulation by including a correction term. This term contains the gradient of σ_j which makes the stochastic component unwieldy and difficult to interpret, and is hence avoided.

The choice of the noise Hamiltonians is up to the practitioner and will vary from application to application. Let us, however, consider a simple example by revisiting the Landau-Lifshitz equation (5). Suppose that there is an uncertainty in the external magnetic field. This could be modeled by including a stochastic term in Eq. (5), i.e., by considering the equation

$$\mathrm{d}s = s \times (\gamma B - \alpha s \times B)\mathrm{d}t + s \times \nabla_s H_1(s) \circ dW(t).$$

Isotropic uncertainty in the external magnetic field can be described, e.g., by $\nabla_s H_1(s) = \tilde{B} \in \mathbb{R}^3$. Anisotropic uncertainty follows from selecting H_1 such that $\nabla_s H_1(s)$ varies with s.

III. PROPOSED SYMPLECTIC INTEGRATORS

In this section, we present the two proposed symplectic integrators for stochastic spin systems in $\mathbb{R}^{3n}$. The numerical integrators are derived from an isospectral integrator for finite-dimensional stochastic matrix LP systems. Efficient structure-preserving integrators for these systems are obtained by applying discrete *Lie-Poisson reduction* to equivariant symplectic integration schemes for canonical Hamiltonian systems. Detailed derivations are given in [5,31] for deterministic and stochastic LP systems, respectively.

The integrators for matrix flows are translated to systems in $\mathbb{R}^3$ as follows. We may identify elements of $\mathfrak{su}(2)$ or $\mathfrak{so}(3)$ with vectors in $\mathbb{R}^3$ through distinct isomorphisms, as described in the Appendix. As a result, the cross product in $\mathbb{R}^3$ between two vectors can be expressed as the matrix commutator between the corresponding matrices. This implies that the evolution of spin systems in $\mathbb{R}^{3n}$ is equivalent to an isospectral flow in $(\mathfrak{su}(2))^n$ or $(\mathfrak{so}(3))^n$. Similarly, one can apply the isomorphisms between these spaces and $\mathbb{R}^3$ to the deterministic [31] and stochastic [5] isospectral integrator to obtain two distinct symplectic implicit midpoint methods for deterministic and stochastic spin systems. These integration schemes are outlined below.

We describe the integration schemes for general spin systems with transport noise [Eq. (10)]. Let $k, k+1$ denote two time levels separated by a fixed step size h, with corresponding numerical solutions $s_{i,k}, s_{i,k+1}$ and let the midpoint between these time levels given by $\tilde{s}_i$. The subscript i denotes the ith spin. For the sake of readability, we define

$$y = h a_i(\tilde{\mathbf{s}}) + h^{1/2} \sum_{j=1}^{M} \sigma(\tilde{s}_i) \xi_k^{i,j}, \tag{11}$$

which encompasses the gradients of the Hamiltonian and noise Hamiltonians at the midpoint $\tilde{s}_i$ and incorporates the step size h. Here $\xi_n^{i,j}$ are independent and identically distributed (i.i.d.) random variables defined as the truncated variable ξ_h below, to accommodate implicit integration [7,32]. The truncated random variable ξ_h is obtained from the random variable $\zeta \sim \mathcal{N}(0,1)$ as

$$\xi_h = \begin{cases} \zeta, & |\zeta| \leqslant A_h \\ A_h, & \zeta > A_h \\ -A_h, & \zeta < -A_h \end{cases}, \tag{12}$$

with $A_h = \sqrt{2|\ln h|}$.

The proposed symplectic implicit midpoint methods for spin systems differ in the adopted definition of the midpoint. The midpoint $\tilde{s}_i$ is found through the implicit equations below, respectively corresponding to the $\mathfrak{su}(2)$ and $\mathfrak{so}(3)$ isomorphisms applied to the isospectral LP integration scheme. The classical implicit midpoint scheme (referred to as IMP) is included for comparison,

$$s_{i,k} = \tilde{s}_i - \tfrac{1}{2}\tilde{s}_i \times y, \tag{13}$$

$$s_{i,k} = \tilde{s}_i - \tfrac{1}{2}\tilde{s}_i \times y - \tfrac{1}{16}(y \times \tilde{s}_i \times y - (y \cdot \tilde{s}_i)y), \tag{14}$$

$$s_{i,k} = \tilde{s}_i - \tfrac{1}{2}\tilde{s}_i \times y + \tfrac{1}{4}(\tilde{s}_i \cdot y)y. \tag{15}$$

Here, the scheme (13) is the classical midpoint method, (14) is obtained via the $\mathfrak{su}(2)$ isomorphism, and (15) via the $\mathfrak{so}(3)$ isomorphism.

For each method, the spin configurations at time level $k+1$ are computed via

$$s_{i,k+1} = s_{i,k} + \tilde{s}_i \times y. \tag{16}$$

Both methods are second-order accurate in the deterministic case. For stochastic systems, the schemes are of weak order 1 and mean-square order 1/2 under the assumption that the drift and diffusion coefficients are sufficiently smooth, C^4 and C^5 respectively. This implies that the integrators are suitable for a large class of Hamiltonians and noise Hamiltonians, facilitating, e.g., the simulation of spin systems with anisotropic stochastic forcing. The corresponding proofs and numerical convergence tests are found in [5]. Both methods are variants of the classical implicit midpoint method and thus preserve the spin magnitude and are self-adjoint. Furthermore, the methods are symplectic [5] when applied to spin systems, in contrast to the standard implicit midpoint method. We refer to these methods as isospectral midpoint methods and denote these by su2IsoMP and so3IsoMP, respectively.

The deterministic so3IsoMP method was originally derived by [33] from an isospectral LP integrator on $\mathfrak{so}(3)$ [31]. The extension of the LP integrator to systems with transport noise [5] has enabled the development of so3IsoMP as currently presented, and it hence possesses the same desirable features as the deterministic variant. First, it is symplectic for any Hamiltonian due to the second-order correction term in (15). Second, it requires only three coordinates and no auxiliary variables, making it a minimal-variable symplectic integrator in $\mathbb{R}^3$ [15]. The su2IsoMP method possesses the same properties. The so3IsoMP method has concurrently and independently been derived from a variational principle [34].

Compared to IMP, both so3IsoMP and su2IsoMP can be implemented without many additional computational costs. The implicit step in IMP requires solving $3n$ nonlinear equations at each time step [28], which is the primary source of computational costs. Evidently, this remains the same for so3IsoMP and su2IsoMP. The second-order corrections that distinguish these methods from IMP are computed efficiently, since these are explicit terms defined separately for each spin.

IV. NUMERICAL EXPERIMENTS

In this section, we present numerical results for both deterministic and stochastic spin systems. In particular, we focus on conservation properties and numerical convergence and compare these to the classical midpoint method and the SIB method [28]. These are illustrated for certain single-spin and multispin systems.

A. Single-spin systems

Two examples of single-spin systems are used to compare su2IsoMP and so3IsoMP to existing methods and to illustrate the symplecticity of the methods.

We first consider a simple example of the deterministic LL equation. For simplicity, we choose s and B such that they are of unit norm. It is then readily verified that the Hamiltonian satisfies $H(s) = s \cdot B = \cos\theta$, where θ denotes the angle between the magnetic moment s and the external field B. Moreover, the dissipative term in Eq. (5) ensures that the Hamiltonian decays as [19]

$$\frac{\mathrm{d}H}{\mathrm{d}t} = -\alpha \|s \times B\|^2 = -\alpha \sin^2\theta. \tag{17}$$

An analytical solution for the evolution θ can be derived from these relations and is given by

$$\theta_0 = \theta(0) = \arccos(s(0) \cdot B),$$
$$\theta(t) = 2\arctan(\tan(\theta_0/2)e^{-\alpha t}). \tag{18}$$

The computed numerical solutions are shown and compared to the analytical solution in Fig. 1, computed with a time step size $h = 0.5$ and a random initial condition. The evolution of θ indicates that su2IsoMP and so3IsoMP accurately capture the dynamics of the magnetic moment. The difference between the computed θ and the analytical solution reveals that su2IsoMP has a decreased phase error, compared to the other methods. Furthermore, the results of IMP and so3IsoMP are virtually indistinguishable. The same qualitative result is observed for the azimuthal angle of the spin, but is not shown here.

The second example is a nonlinearly perturbed spinning top [15] where one can distinguish between symplectic and nonsymplectic methods. The deterministic single-spin equation is solved numerically, adopting the Hamiltonian

$$H_{\mathrm{NLST}}(s) = \frac{1}{2}\sum_{j=1}^{3}\frac{1}{I_j}\left(s_j^2 + \frac{2}{3}s_j^3\right), \quad I = (1, 2, 4). \tag{19}$$

Note that the subscripts j denote the components of the spin. A time step size $h = 1$ is employed with a randomly selected initial condition, which is the same for all methods. The simulation results in Fig. 2 show that the symplectic su2IsoMP method retains the periodic trajectory of the spin, whereas IMP shows nonperiodic behavior. The departure of the Hamiltonian over time shows the expected behavior for symplectic and nonsymplectic methods. The Hamiltonian is not quadratic hence it is not conserved under IMP and instead a linear drift is observed. The su2IsoMP and so3IsoMP methods are symplectic, and the observed energy departure is thus nonzero but bounded [35].

Similar qualitative behavior may be observed when including a stochastic perturbation of small magnitude. To demonstrate this, we introduce the noise Hamiltonians

$$H_j(s) = 10^{-3}s_j, \tag{20}$$

which is interpreted as isotropic noise in the field acting on the magnetic moment s. In this case, the trajectories are no longer periodic, even when computed with the symplectic integrators. A clear difference between the trajectories arises in long-time simulations, depicted in Fig. 3 for IMP and su2IsoMP. The symplectic methods approximately retain the trajectory of the deterministic system (Fig. 2), which is also reflected in a bounded deviation of the Hamiltonian. On the other hand, the drift in the Hamiltonian is still observed for IMP. The solution trajectory drifts significantly from the deterministic trajectory until it reaches an approximately periodic solution markedly different from the solution of su2IsoMP.

B. Heisenberg spin chain

In this section, we demonstrate numerically certain properties of the integrators in multispin systems via simulations of the Heisenberg spin chain.

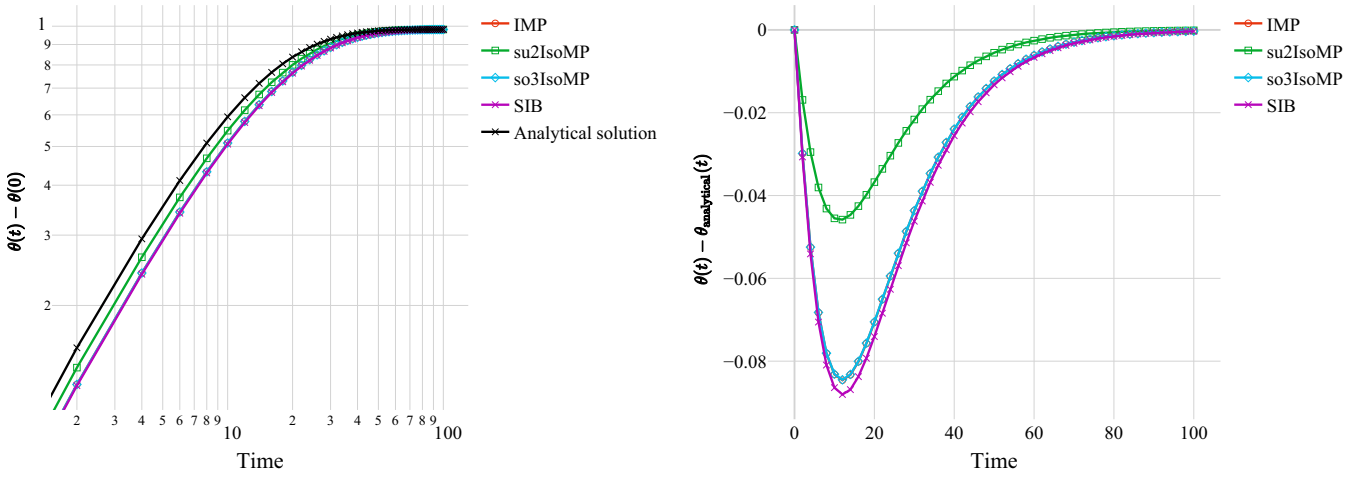

FIG. 1. Comparison of different methods for the deterministic LL equation. Left: evolution of the angle θ between the magnetic moment and the external field over time. Note that the results of IMP, so3IsoMP, and SIB are virtually indistinguishable in this panel. Right: difference between the numerically predicted θ and the analytical solution. In this panel, the results of IMP and so3IsoMP lie on top of each other and cannot be distinguished.

The total spin is a conserved quantity in the deterministic Heisenberg spin chain. Conservation of total spin has been proven for IMP [28] due to the structure of the numerical method. This structure is the same for su2IsoMP and so3IsoMP and hence they inherit this conservation property. Furthermore, since the proof does not assume a specific coupling of different spins or the relative location of these spins, the conservation property is trivially extended to include next-nearest neighbor interactions, interactions over arbitrary distances, and two-dimensional and three-dimensional systems. In these cases, the expression for the Hamiltonian becomes more intricate but the governing equations do not change. For that reason, we demonstrate here the stochastic one-dimensional Heisenberg spin chain with nearest- and next-nearest-neighbor interactions.

The conservation of total spin is illustrated numerically in the left panel of Fig. 4, showing the absolute departure over time. Throughout the simulation, the implicit midpoint methods conserve the total spin up to machine accuracy without drift. This particular example was computed for $n = 100$ spins, with interaction strengths $J_{\text{nn}} = 1$ and $J_{\text{nnn}} = 1/4$ and a time step size $h = 0.25$.

To illustrate the order of convergence of the numerical methods, we consider the stochastic Heisenberg spin chain with nearest-neighbor interactions and damping. That is, we consider the Hamiltonian (6) and define, largely following [28],

$$a_i(\mathbf{s}) = -\nabla_{s_i} H(\mathbf{s}) - \alpha s_i \times \nabla_{s_i} H(\mathbf{s}), \tag{21}$$

$$\sigma(x)y = -\sqrt{2D}y - \alpha\sqrt{2D}x \times y, \tag{22}$$

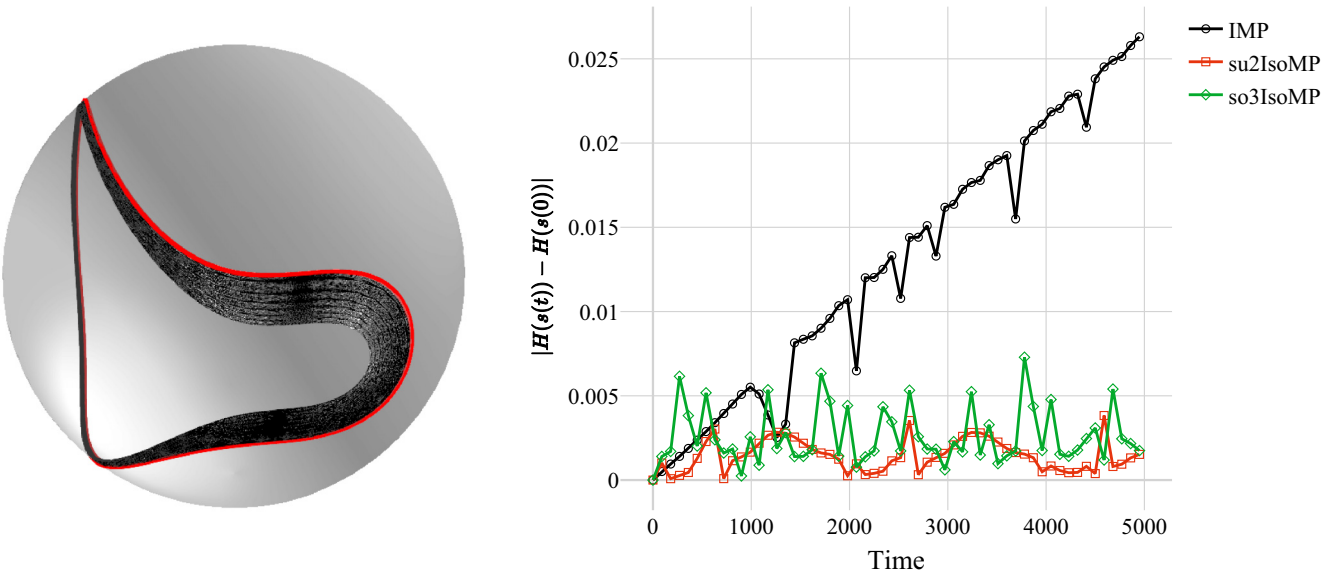

FIG. 2. Results for the single-spin system with Hamiltonian (19). Left: trajectories obtained with IMP (black) and su2IsoMP (red). Right: departure of the Hamiltonian over time.

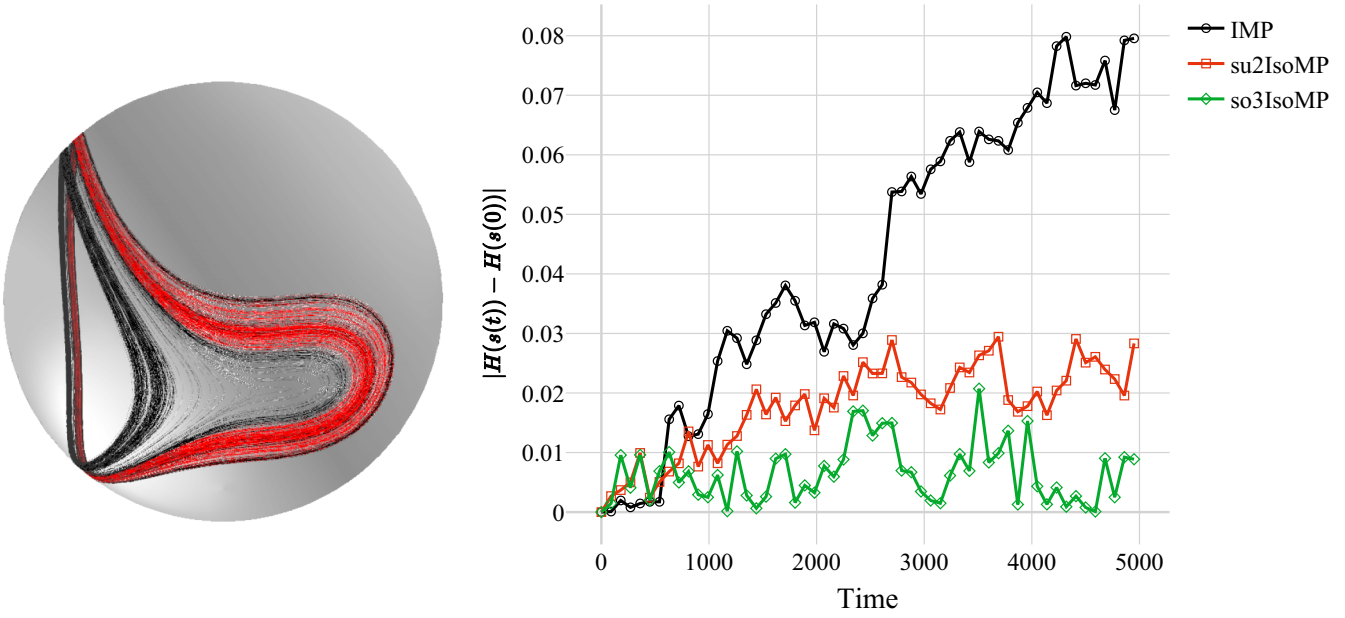

FIG. 3. Results for the single-spin system with deterministic Hamiltonian (19) and noise Hamiltonians (20). Left: trajectories obtained with IMP (black) and su2IsoMP (red). Right: departure of the Hamiltonian over time.

where we choose $D = \alpha/(1+\alpha^2)$. We adopt an exchange parameter $J_{\mathrm{nn}} = 1$ and a damping $\alpha = 0.1$ for a total of $n = 100$ spins. We compute the reference result from stochastic realizations with step size $h_{\mathrm{ref}} = 2^{-25} \approx 2.98 \times 10^{-8}$ and choose the coarse time step sizes as $h_{\mathrm{ref}} \cdot 2^3, \ldots, h_{\mathrm{ref}} \cdot 2^8$. A total of 100 independent realizations are compared to the reference at 16 times the largest considered step size. We employ the definition of the strong error,

$$\mathbb{E}[\|\mathbf{s}(hk) - \mathbf{s}_{k,\mathrm{ref}}\|^2]^{1/2}, \tag{23}$$

where $\mathbf{s}(hk)$ denotes the numerical solution after hk time units and $\mathbf{s}_{k,\mathrm{ref}}$ is the reference solution at the same time instance. The norm $\|\cdot\|$ is the standard two-norm for vectors in $(\mathbb{R}^3)^n$. The strong errors for the stochastic Heisenberg spin chain are shown in the right panel of Fig. 4, from which the expected order 1/2 convergence is observed. The order of convergence was only observed at sufficiently small step sizes. At these values of h, all adopted methods produce nearly identical results.

V. CONCLUSIONS AND OUTLOOK

In this paper, we presented two symplectic integrators for stochastic spin systems, labeled su2IsoMP and so3IsoMP. The numerical methods are variants of the classical implicit midpoint method, where the midpoint is defined differently through the inclusion of a second-order correction. Both methods are derived from a stochastic isospectral Lie-Poisson integrator on the matrix algebras $\mathfrak{su}(2)$ and $\mathfrak{so}(3)$. Identifying spin systems in $\mathbb{R}^3$ with these isospectral Lie-Poisson systems

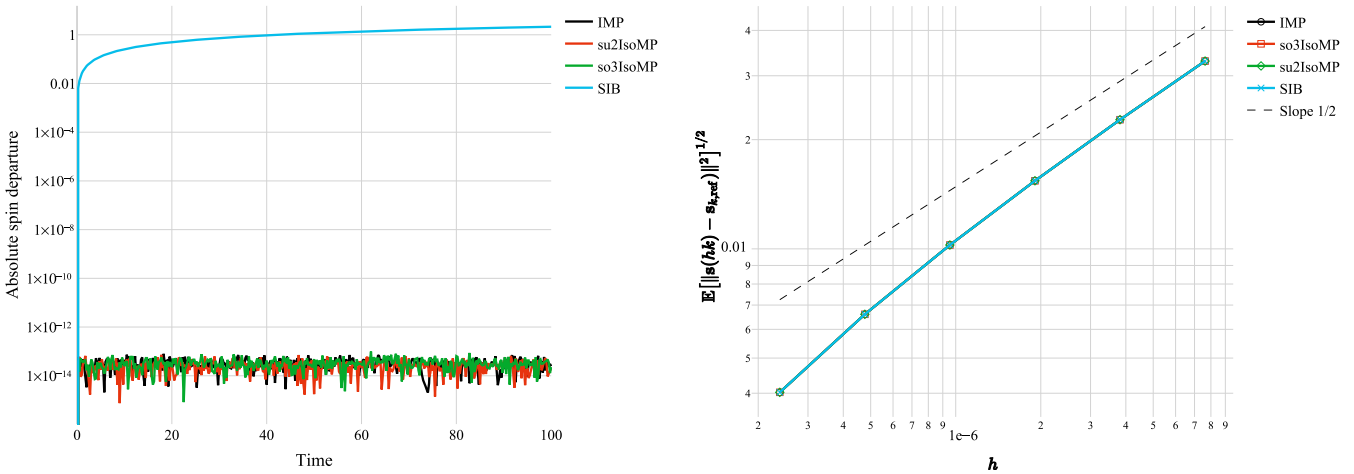

FIG. 4. Left: departure of the total spin for the deterministic Heisenberg spin chain with nearest-neighbor and next-nearest-neighbor interactions. Right: Strong errors for the stochastic Heisenberg spin chain with only nearest-neighbor interactions, using 100 independent realizations.

allowed for a reformulation of the structure-preserving integrator for matrix flows as two distinct numerical schemes for spin systems. The two integrators thereby inherited favorable properties such as symplecticity and applicability to a large class of stochastic forcing functions.

A possible extension of the methods presented in this paper concerns the application to temporally nonlocal dynamics. First, a fruitful development would be to address the simulation of time-dependent Hamiltonians, observed, e.g., when including inertia effects in the dynamics [36]. Second, semimartingales as the driving stochastic processes is compatible transport noise [37] and provides a natural progression to include different types of stochasticity without breaking the conservation properties of the governing equations. Both extensions require additional method development and corresponding analysis.

Further work should be dedicated to computationally efficient adaptations of these methods. The methods proposed in this paper are both implicit midpoint methods that require solving a system of nonlinear equations. Their performance should be compared to existing methods in computationally challenging and physically relevant test cases. Semi-implicit variants of su2IsoMP and so3IsoMP may additionally be studied, similar to the SIB method [28]. Here, one may take existing explicit or semi-implicit Lie-Poisson integrators for isospectral matrix flows and convert these to integrators for spin systems, ideally maintaining desirable geometric properties of the Lie-Poisson system.

ACKNOWLEDGMENTS

We wish to express our gratitude to K. Modin and E. Luesink for the valuable input and insightful discussions that helped improve the paper. The computations were enabled by resources provided by Chalmers e-Commons at Chalmers as well as by resources provided by the National Academic Infrastructure for Supercomputing in Sweden (NAISS), partially funded by the Swedish Research Council through Grant Agreement No. 2022-06725. This work was supported in part by the Swedish Research Council (VR) through Grant No. 2022-03453, by the Wallenberg AI, Autonomous Systems and Software Program (WASP) funded by the Knut and Alice Wallenberg Foundation.

DATA AVAILABILITY

The data that support the findings of this article are openly available [38]; embargo periods may apply.

APPENDIX: ISOMORPHISMS BETWEEN $\mathbb{R}^3$ AND $\mathfrak{su}(2)$, $\mathfrak{so}(3)$.

In this Appendix, we elaborate on the translation between isospectral matrix flows and spin systems.

1. The $\mathfrak{su}(2)$ case

Let $z = (z_1, z_2, z_3)^T \in \mathbb{R}^3$. We define the isomorphism $\phi_{\mathfrak{su}(2)}$ between $\mathbb{R}^3$ and $\mathfrak{su}(2)$ as

$$\phi_{\mathfrak{su}(2)} : \mathbb{R}^3 \to \mathfrak{su}(2),$$
$$\phi_{\mathfrak{su}(2)}(z) = \frac{1}{2}\begin{bmatrix} iz_3 & z_2 + iz_1 \\ -z_2 + iz_1 & -iz_3 \end{bmatrix}. \tag{A1}$$

We additionally define the function $y : \mathbb{R}^3 \to \mathbb{R}^3$ and adopt the notation $Z = \phi_{\mathfrak{su}(2)}(z)$ and $Y = \phi_{\mathfrak{su}(2)}(y(z))$. It is then readily verified that the isospectral system in $\mathfrak{su}(2)$,

$$\dot{Z} = [Y, Z], \tag{A2}$$

is equivalent to the system of equations

$$\dot{z} = z \times y \tag{A3}$$

in $\mathbb{R}^3$. Applying the inverse of $\phi_{\mathfrak{su}(2)}$ to the isospectral midpoint method [[5], Sec. 4.3] yields the integration scheme (14).

2. The $\mathfrak{so}(3)$ case

We consider $z \in \mathbb{R}^3$ and $y : \mathbb{R}^3 \to \mathbb{R}^3$ as defined in Eq. (A1). We define the isomorphism $\phi_{\mathfrak{so}(3)}$ between $\mathbb{R}^3$ and $\mathfrak{so}(3)$ as

$$\phi_{\mathfrak{so}(3)} : \mathbb{R}^3 \to \mathfrak{so}(3),$$
$$\phi_{\mathfrak{so}(3)}(z) = \begin{bmatrix} 0 & z_3 & -z_2 \\ -z_3 & 0 & z_1 \\ z_2 & -z_1 & 0 \end{bmatrix}. \tag{A4}$$

Adopting $Z = \phi_{\mathfrak{so}(3)}(z)$ and $Y = \phi_{\mathfrak{so}(3)}(y(z))$, we find that $\dot{Z} = [Y, Z]$ is equivalent to $\dot{z} = z \times y$. Similarly, we find that applying the inverse of $\phi_{\mathfrak{so}(3)}$ to the isospectral midpoint method [[5], Sec. 4.3] yields the integration scheme (15).

[1] E. Hairer, M. Hochbruck, A. Iserles, and C. Lubich, Oberwolfach Rep. **3**, 805 (2006).
[2] J. Hong, J. Ruan, L. Sun, and L. Wang, arXiv:2006.03880.
[3] C.-E. Bréhier, D. Cohen, and T. Jahnke, Math. Comput. **92**, 2167 (2023).
[4] E. Luesink, S. Ephrati, P. Cifani, and B. Geurts, Adv. Contin. Discrete Models **2024**, 1 (2024).
[5] S. Ephrati, E. Jansson, A. Lang, and E. Luesink, arXiv:2408.16701.
[6] C. A. Anton, Y. S. Wong, and J. Deng, Int. J. Numer. Anal. Model. **11**, 166 (2014).
[7] G. N. Milstein, Y. M. Repin, and M. V. Tretyakov, SIAM J. Numer. Anal. **40**, 1583 (2002).
[8] N. Bou-Rabee and H. Owhadi, IMA J. Numer. Anal. **29**, 421 (2009).
[9] D. D. Holm and T. M. Tyranowski, BIT Numer. Math. **58**, 1009 (2018).
[10] O. Eriksson, A. Bergman, L. Bergqvist, and J. Hellsvik, *Atomistic Spin Dynamics: Foundations and Applications* (Oxford University Press, Oxford, 2017).
[11] D. D. Holm, Proc. R. Soc. London, Ser. A **471**, 20140963 (2015).

[12] R. Steinigeweg and H.-J. Schmidt, Comput. Phys. Commun. **174**, 853 (2006).
[13] T. Arponen and B. Leimkuhler, BIT Numer. Math. **44**, 403 (2004).
[14] J. Frank, W. Huang, and B. Leimkuhler, J. Comput. Phys. **133**, 160 (1997).
[15] R. I. McLachlan, K. Modin, and O. Verdier, Phys. Rev. E **89**, 061301(R) (2014).
[16] J. Marsden and A. Weinstein, Rep. Math. Phys. **5**, 121 (1974).
[17] M. Lakshmanan, Philos. Trans. R. Soc. A **369**, 1280 (2011).
[18] T. L. Gilbert, IEEE Trans. Magn. **40**, 3443 (2004).
[19] A. Bloch, P. Krishnaprasad, J. E. Marsden, and T. S. Ratiu, Commun. Math. Phys. **175**, 1 (1996).
[20] P. Depondt and F. Mertens, J. Phys.: Condens. Matter **21**, 336005 (2009).
[21] E. Y. Vedmedenko, H. P. Oepen, A. Ghazali, J.-C. S. Lévy, and J. Kirschner, Phys. Rev. Lett. **84**, 5884 (2000).
[22] M. E. Gouva, G. M. Wysin, A. R. Bishop, and F. G. Mertens, Phys. Rev. B **39**, 11840 (1989).
[23] A. R. Völkel, F. G. Mertens, A. R. Bishop, and G. M. Wysin, Phys. Rev. B **43**, 5992 (1991).
[24] B. Skubic, J. Hellsvik, L. Nordström, and O. Eriksson, J. Phys.: Condens. Matter **20**, 315203 (2008).
[25] V. P. Antropov, M. I. Katsnelson, B. N. Harmon, M. van Schilfgaarde, and D. Kusnezov, Phys. Rev. B **54**, 1019 (1996).
[26] D. Cohen and G. Vilmart, Int. J. Comput. Math. **99**, 4 (2022).
[27] J. L. García-Palacios and F. J. Lázaro, Phys. Rev. B **58**, 14937 (1998).
[28] J. Mentink, M. Tretyakov, A. Fasolino, M. Katsnelson, and T. Rasing, J. Phys.: Condens. Matter **22**, 176001 (2010).
[29] M. Émery, *Séminaire de Probabilités XXIV 1988/89* (Springer, Berlin, Heidelberg, 2006), pp. 407–441.
[30] P. E. Kloeden and E. Platen, *Stochastic Differential Equations* (Springer, Berlin, Heidelberg, 1992).
[31] K. Modin and M. Viviani, Found. Comput. Math. **20**, 889 (2020).
[32] G. N. Milstein and M. V. Tretyakov, *Stochastic Numerics for Mathematical Physics* (Springer, Berlin, Heidelberg, 2004), Vol. 39.
[33] M. Viviani, BIT Numer. Math. **60**, 741 (2020).
[34] F. Gay-Balmaz and M. Wu, arXiv:2412.19368.
[35] B. Leimkuhler and S. Reich, *Simulating Hamiltonian Dynamics* (Cambridge University Press, Cambridge, UK, 2004), Vol. 14.
[36] S. Bhattacharjee, L. Nordström, and J. Fransson, Phys. Rev. Lett. **108**, 057204 (2012).
[37] O. D. Street and D. Crisan, Proc. R. Soc. London, Ser. A **477**, 20200957 (2021).
[38] https://doi.org/10.5281/zenodo.14505559.